

Structural and Running Safety Assessment of the Handling and Distributing System in Automated Container Terminal Considering Container Vehicle-Truss Bridge Coupled Vibration

Lu Kai-liang¹, Yan Wei², Ye Hao³, Bao Yan⁴ and Liu Xiang-rui⁵

^{*1,2,3,4} Logistics Engineering College, Shanghai Maritime University
⁵ Shanghai General Motors Co. Ltd.

lkl1984@163.com

Abstract

This paper introduces a scheme of constructing a three-dimensional container handling and distributing system between crane yard and storage yard for the efficient, smart, energy-saving automated container terminal (ACT). This scheme can effectively solve the problem that the AGVs in existing ACT should give way to each other in ground planer transportation mode, and has advantages of lower investment cost higher handling efficiency. The safety and running stationarity of the container vehicle-truss bridge structure greatly affects the ACT's efficiency and lifespan. The assessment criteria for structural security and running stationarity was put forward first. By utilizing free-interface component mode synthesis (CMS) method, the coupled vibration time-domain responses, inspired by self-excitation including track irregularity and hunting movement as well as wind and seismic load, were obtained. Accordingly, the structural and running stationarity were assessed by indicators such as deflection-span ratio, vibration acceleration, wheel-rail relative displacement, suggesting a speed threshold of container vehicle under seismic and operational wind loads. The simulation and model test results also validate lead rubber bearing (LRB)'s effects on vibration isolation and absorption, thus can increase ground motion intensity and vehicle speed thresholds to structural safety.

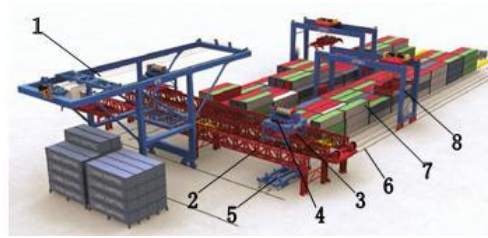
Keywords: Automatic Container Terminal, Container Vehicle-Truss bridge Coupled Vibration, Structural Safety Assessment, Running Safety Assessment, Free-interface Component Mode Synthesis, Model Test

1. Introduction

Through investigation into automation and informatization of the container terminals all over the world, container transportation between crane yard and storage yard is implemented usually by AGVs, which have many drawbacks, such as, high capitalized cost, low efficiency, and serious interference among AGVs.

To resolve these problems, a three-dimensional container handling and distributing system is proposed between crane yard and storage yard (as shown in Figure 1). The system comprises container crane, container vehicle-truss bridge system, and ground track, ground rotary container vehicle. Container distribution procedure is described as follows and vice versa: firstly, crane 1 lifts one container from one vessel to one container transport vehicle 3 seated on the truss bridge 2. Secondly, the transport vehicle 3 runs and reaches certain position in high speed and then lifted down to one ground rotary container vehicle 4 by one

lifting vehicle 5. Thirdly, the ground vehicle 4 with one container drives to the storage yard 7 on the track 6.



1. container crane; 2. truss bridge; 3. container transport vehicle; 4. container lifting vehicle; 5. ground rotary container vehicle; 6. ground track; 7. yard; 8. track crane

Figure 1. Virtual Reality Simulation for Automated Container Terminal (ACT)

Compared to the existing ACTs, this scheme possesses many advantages as follows: (1) Three-dimensional transportation replaces the ground planer way, solving the AGVs' interference problem. (2) The container vehicle no longer depends on GPS navigation and positioning system, instead, it adopts a more convenient and more accurate orbital positioning. (3) The container vehicle and truss bridge distribution system is less expensive than the AGV system. (4) Making it available to handle two FEUs at the same time. Last but not the least, green power drive of the entire process is utilized and thus reduce the operating cost.

In this scheme, structural safety and running stability of the core system, that is container vehicle-truss bridge, dominates the efficiency of the handling and distributing system. Generally speaking, safety assessment for bridge structure mainly includes: (1) Evaluation of bearing capacity: bridge structure in the aspects of strength, stiffness, stability, whether or not to meet the existing transport load requirements. (2) Durability assessment: fatigue damage and remaining life so far. (3) Applicability evaluation: travelling safety, running stationarity, and passenger comfort, *etc.*, [1-10]. At present, bridge safety assessment methods mainly include: (1) Survey method based on the appearance; (2) Expertise evaluation method; (3) Analytic hierarchy process; (4) Fuzzy comprehensive evaluation method; (5) Methods based on the theory of structural reliability; (6) Method based on damage mechanics and fatigue fracture; (7) Methods based on design specification, *etc.*, [11-12]. In order to assess the quality of the structural safety and operation stability, the coupled vibration responses of the vehicle system should be figured out first.

Vehicle and bridge coupled vibration research has been focusing on the area of rail transportation [1-6]. Factors which affect the vibration of vehicle-bridge (V&B) system, can be classified into self-excitation (track irregularity and hunting movement, *etc.*) and external excitation (wind and seismic load, *etc.*). Now multi-rigid body-spring-damper discrete model is commonly adopted as the vehicle model while FEM model is applied to bridge model. Then the system equation is formed through wheel-rail interaction. The solution of the equation is in the time domain due to time-varying.

Wind and seismic loads are two crucial external excitations of V&B system. Many researchers have deployed research on the V&B system coupled vibration issues, such as long-span cable stayed bridges or suspension bridges, under disturbing wind [1-5] or seismic circumstances [6]. Analysis of the wind or earthquake effect on vertical and lateral vibration was presented and safe speed limit was calculated. The free-interface component mode synthesis (CMS) is the most comprehensively conducted on the issue because of high efficiency and convenient combination with the experimental modal technique. Interface

(force and displacement) compatibility conditions can commensurate approximately with wheel-rail interaction. Thus vehicle and bridge are combined together to one entire system for coupled vibration analysis [1-3, 7, 8]. Moreover, it reduces the degree of freedom for the system with further step as well as enhances the efficiency of the calculation.

This paper applies double coordinate free-interface CMS method to solve and verify the issues on the coupled vibration time-domain responses under the irregularity and hunting movement as well as wind and seismic load of the three-dimensional handling and distributing system in the ACT, and evaluates the structural safety, running safety and stability. Results of the research are qualified to serve as the theoretical basis for health monitoring, lifetime prediction, and optimization design as well as the establishment of the industrial standard of ACT's infrastructure.

2. Structural and Running Safety Assessment Criteria

The braces and truss beams of the bridge are linked in full rigid (weld and bolt connection) or LRB connected way (full flexible support). Overall size of the truss bridge is shown in Figure 2.

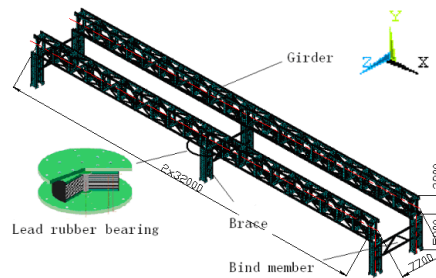


Figure 2. Schematic Diagram of the Truss Bridge (double-span-single-line)

The container vehicle-truss bridge system is a newly sprouted design, and there are no specially formulated standards or specifications designed for this system, while its structural safety assessment apply reference of the railway bridge standards as norms.

2.1. Bridge Safety Assessment Standards

a. Deflection-span ratio threshold: for continuous truss bridges referring to “*Railway Bridge and Culvert Design Basic Specifications*”, vertical deflection caused by a moving train must be lower than $L/900$, where L is the span. But lateral limitation is not provided (refer to TB10002.1-99). Japan's truss bridge specification takes the half of the vertical deflection as the lateral value, which is less than $L/1800$. As for the truss bridge here, vertical and horizontal deflections are 0.036m and 0.018m respectively.

b. Acceleration threshold: EUROCODE indicates the vertical acceleration maximum must be less than 0.5g, and “*Railway Bridge Verification Specification*” specifies the limitation of lateral acceleration as 1.4m/s^2 (0.14g) during the train is passing through.

2.2. Vehicle Running Safety Assessment Standards

Running safety is evaluated by the derailment coefficient, wheel load reduction rate and wheel transverse rocking force at present. This paper uses this derailment geometric criteria as evaluation. The rules are as follows: (1) Amount of wheel suspension $|\mu_s|$ equals to the

suspension $|\mu_s|$ when top of the rim climb up to the upper apex of the rail. (2) And lateral displacement $|\Delta|$ of wheel relative to the rail $|\Delta|$ equals to the lateral displacement $|\Delta|$ when top of the rim climb up to the upper apex of the rail. The wheel will run out of the rail when both conditions are satisfied. In this case, $|\mu_s|$ and $|\Delta|$ can be determined as 25mm and 37.5mm by the wheel-rail contact relationship.

2.3. Running Stationarity Assessment Standards

Running stationarity of the vehicle can be evaluated by the indices of vehicle body acceleration. GB5599-85 suggests that vertical and lateral acceleration limit of the train body is lower than 0.7g and 0.5g respectively.

3. Container Vehicle-truss Bridge coupled Vibration Analysis

3.1. Container Vehicle-truss Bridge coupled Vibration Equation

The container vehicle and the low truss bridge finite element method (FEM) model were established. Every truss bridge and each vehicle are divided into free-interface subcomponents. Track model is not established and wheel degree of freedoms (DOFs) as well as rail DOFs are considered as the interface freedoms respectively.

LRB is a common device for seismic isolation and energy consumption, which has its own merits of simple structure, easy manufacture, and convenient installation and so on. Because of LRB's complicated non-linear characteristic, researchers usually adopt the equivalent linear model or the bilinear model in current analysis and design. According to the equivalent linear model, mechanical characteristic parameters of the LRB are listed in Table 1, LRB can be regarded as free-interface substructure.

Table 1. Mechanical Characteristic Parameters of the LRB

Type	Mass m (kg)	Vertical Stiffness K_v (N/m)	Equivalent Horizontal Stiffness k_b (N/m)
GZY300	56	1.188×10^6	1.13×10^3
GZY400	126	1.85×10^6	1.69×10^3
GZY500	228	1.972×10^9	1.91×10^6

Assuming that: (1) Wheel is a rigid body which always contacts with rail, that means, the wheels do not hung up; (2) Small displacement vibration of both vehicle and bridge; (3) Neglecting effect from vehicle longitudinal movement on the bridge vibration and vehicle velocity. According to free-interface CMS method, structure V of any vehicle subcomponents interface compatible conditions are utilized to assembly container vehicle-truss bridge coupled vibration system equation under modal coordinates ${}^V p$.

$${}^V \bar{m} \ddot{{}^V p} + {}^V \bar{c} \dot{{}^V p} + {}^V \bar{k} {}^V p = {}^V \bar{F} \quad (1)$$

Furthermore, assuming that there is no relative displacement between rail and truss beam, considering self-excitation (track irregularity and lateral hunting movement), thus the bridge interface displacement meets

$${}^B u_j = {}^B u_{v_j} + u_{h_j} + u_{s_j} \quad (2)$$

In this equation, ${}^B\mathbf{u}_{v,j}$, $\mathbf{u}_{h,j}$, $\mathbf{u}_{s,j}$ are the bridge interface displacement, wheel set hunting movement and track irregularity vectors respectively .

3.2. Numerical Simulation of Track Irregularity Stochastic Processes

By considering of weak correlation between different directions between track irregularity and wind load, the Shinozuka's method [10] was utilized to simulate one-variant multidimensional homogeneous process, and results in track spectrums which contain left track (LT) and right track (RT) lateral and vertical irregularity, as shown in Figure 3. Moreover, PSD of simulated sample is observed to agree with the target, one example is as shown in Figure 4.

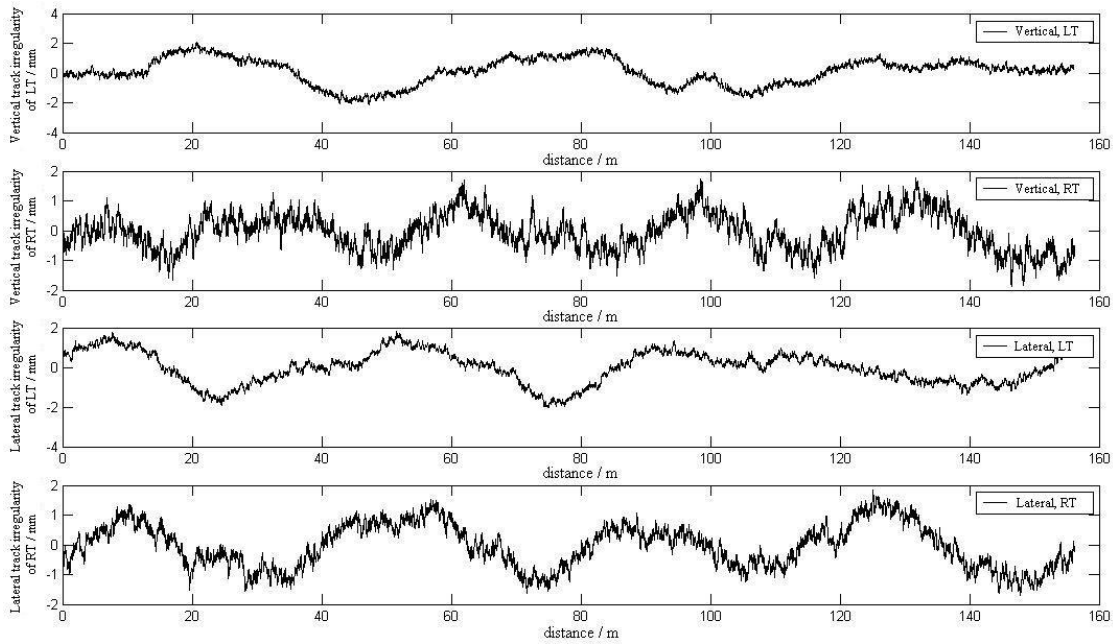


Figure 3. Vertical or Lateral Track Irregularity Curve of the Left and Right Track

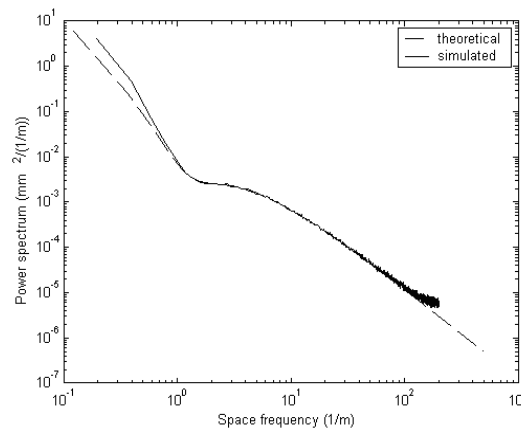


Figure 4. Comparison of the Theoretical and Spectrum and the Simulated Spectrum of the Left Track's Vertical Irregularity

3.3. Self-excitation Vibration Simulation and Model Test Validation

According to P theorem dimensional method, the simulated condition of the structural dynamic model has been derived for analysis, and devise a simulated model, whose geometric ratio of similitude is 1:30 to the real one. The designed model is shown in Figure 5.



Figure 5. Photos of the Truss Bridge and the LRB Models

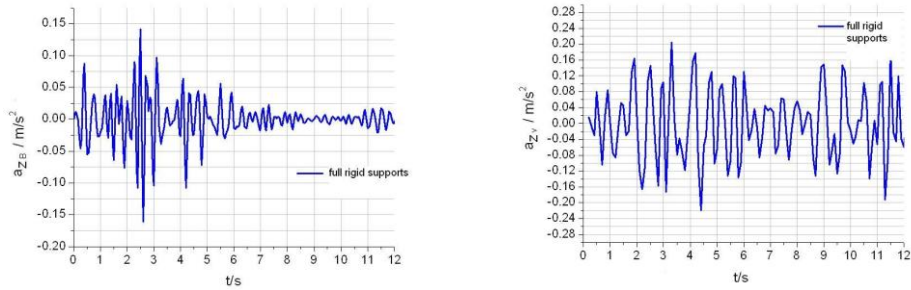
With full rigid or flexible support constraint, acceleration experiment of self-excitation for the coupled vibration system response model and simulation values are listed in Table 2.

Table 2 presents the fact that response of model test acceleration and simulation value agree with each other very well. The vehicle-bridge response value increases with vehicle velocity. Moreover, under full flexible support, the responses are obviously less than that under full rigid supports, indicating that the LBR can effectively reduce the acceleration response.

Table 2. Maximum Acceleration Response Comparison of Model Test and Prototype Simulation

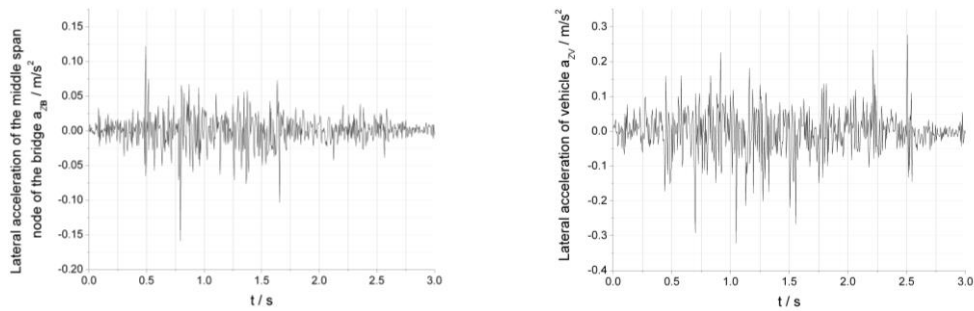
Prototype Vehicle Speed (m/s)	Support Form	Maximum Acceleration Response of Bridge (m/s^2)				Maximum Acceleration Response of Vehicle (m/s^2)			
		Vertical		Lateral		Vertical		Lateral	
		Test	Simulation	Test	Simulation	Test	Simulation	Test	Simulation
4	rigid	2.05	1.54	0.15	0.16	0.26	0.069	0.32	0.220
	flexible	1.37	1.32	0.14	0.12	0.22	0.063	0.29	0.218
6	rigid	2.07	1.60	0.20	0.20	0.38	0.129	0.61	0.410
	flexible	1.70	1.34	0.16	0.15	0.41	0.126	0.48	0.397
8	rigid	2.23	1.65	0.19	0.24	0.49	0.223	0.81	0.634
	flexible	1.80	1.38	0.18	0.20	0.55	0.238	0.73	0.576

When the vehicle runs at the speed of 4m/s during single running, lateral acceleration of the middle span of the bridge with full rigid supports and vehicle acceleration, lateral acceleration response prototype simulation and model test time-history curves of the truss bridge and the vehicle are shown in Figure 6 and Figure 7.



a) Lateral acceleration of the bridge middle span b) Lateral acceleration of the vehicle

Figure 6. Lateral Acceleration Response Prototype Simulation Time-history Curves ($v_V=4\text{m/s}$)



a) Lateral acceleration of the bridge middle span b) Lateral acceleration of the vehicle

Figure 7. Lateral Acceleration Response Model Test Time-history Curves ($v_V=4\text{m/s}$)

By comparing Figure 6 with Figure 7, the vehicle-bridge vibration waveforms are commensurate well with the simulation. Prototype simulation and model test results verify that the model design is reasonable and Dual-compatible CMS method is feasible to solve the coupled vibration of the vehicle-bridge system.

3.4. Wind Field Simulation and Wind Load Calculation

In this paper, the numerical simulation method, which is identical to track irregularity, generates wind speed time history from wind power spectrum, and wind load is obtained on the basis of the relationship between wind velocity and pressure. Along-wind adopts Kaimal spectrum.

$$S_w(y, n) = \frac{200f \cdot u_*^2}{n(1 + 50f)^{5/3}} \quad (3)$$

Adopting Lumley-Panofsky spectrum to tackle vertical-wind

$$S_v(y, n) = \frac{3.36f \cdot u_*^2}{n(1 + 10f^{5/3})} \quad (4)$$

In the Equations (3) and (4): n denotes frequency (Hz); $f = ny / \bar{U}(y)$; u_* denotes shear velocity, m/s.

$$u_* = 0.4\bar{U}(y) / \ln(y / y_0) \quad (5)$$

Where, height y , m; ground roughness y_0 , m; mean velocity $\bar{U}(y)$ at y height.

When $\bar{U}(y)=60\text{m/s}$, along-wind and vertical-wind velocity time-history curves of V&B are illustrated in Figure 8.

The wind load F_{wind} consists of resistant force F_D , lifting force F_L and torque force F_M . Every component includes static load caused by mean wind, buffeting load caused by fluctuating wind, and self-excitation force caused by the wind-vehicle-bridge interaction. Static load is an invariant component expressed by dynamic pressure, invariant coefficient and structure characteristic dimensions. Also, buffeting force can be treated as invariant load expressed by the Scanlan's aerodynamic expression [4, 5]. However, the self-excitation force is a variant one, function of structural displacement and velocity, reflecting the interaction of wind and structure. In this paper, the last load is neglected.

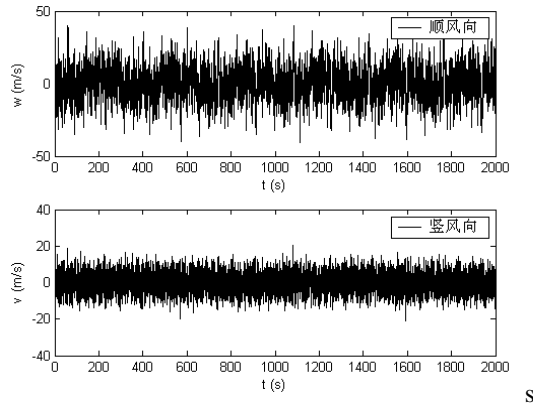


Figure 8. Time History of Along-wind and Vertical-wind Fluctuating Wind Velocity ($\bar{U}(10) = 60\text{m/s}$)

The static load applied on structure of unit length can be expressed as

$$F_D = \frac{1}{2} \rho \bar{U}^2 C_D H, \quad F_L = \frac{1}{2} \rho \bar{U}^2 C_L B, \quad F_M = \frac{1}{2} \rho \bar{U}^2 C_M B^2 \quad (6)$$

Where, ρ is the air density, \bar{U} denotes the designed wind mean velocity, H , B denote the structure height and width respectively; C_D , C_L and C_M is resistant, lifting and torque coefficients affected by section shape, flow direction and determined by relevant references or wind tunnel test. When the length of the structure is not significant, all the aerodynamic coefficients can be assumed constant along the length direction.

The truss bridge is in girder construction, regarding C_D as 1.6 by “Rules for Designing Cranes”, $C_L = 0.2$ and $C_M = 0.1$ referring to “Guidelines for designation of Highway Bridge Wind Resistance”. Wind area of the vehicle is not qualified for considering its wind load, due to the majority of wind load focuses on the container as well as the negligence of lifts and moments, and only takes resistance into accounts. Aerodynamic damping is generally far less than the structure damping, if the average wind velocity equals 60m/s, the truss bridge damping only accounts for 5548N·s/m, which is greatly less than its structure damping, thus can be neglected.

3.5. Vehicle-bridge coupled Vibration Response under Seismic and Operational Wind Load

(1) Vehicle-bridge coupled vibration response under wind load

When the vehicle runs in single line, the response of the system under the full rigid supports is illustrated in Figure 9. The first 600 seconds is the stage under wind load only and later is the stage of the coupled vibration.

According to Figure 9, the wind load of truss bridge has little effect on vertical displacement, because firstly the mainstream of the wind direction is horizontal while wind of vertical load is small; Secondly vertical wind resistance and lift will counteract each other in part. Wind load influence mainly on the lateral dynamic response of the truss bridge. The wind exerts little effect on the vertical acceleration of the vehicle. The vehicle lateral acceleration response time-history is shown in Figure 10.

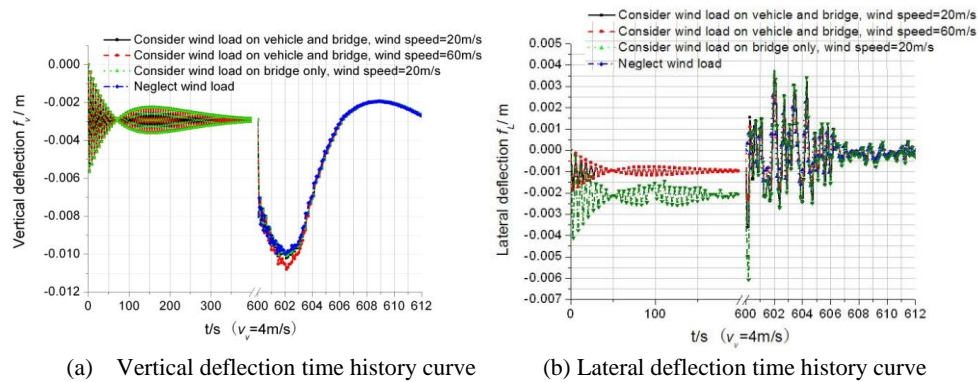


Figure 9. Displacement Response Time-history Curves of the Bridge Middle Span ($v_v=4m/s$)

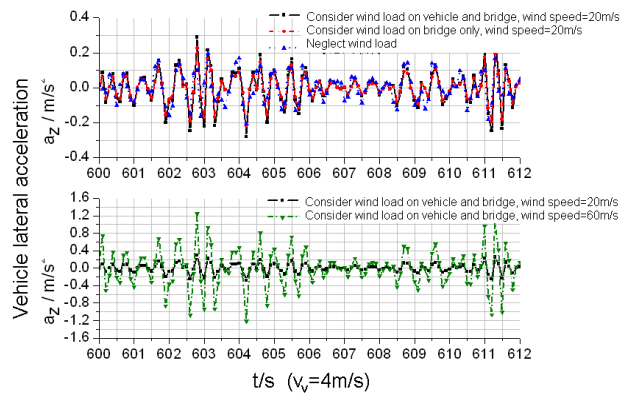


Figure 10. Lateral Acceleration Response Time-history Curves of the Vehicle ($v_v=4m/s$)

Both Figure 10 and Figure 11 indicate that self-excitation is the main factor of the entire vehicle-bridge system vibration. Here, wind load only amplifies the vibration amplitude, which differs from that wind load is the main factor to induce the lateral vibration of long-span high-speed railway bridge [2, 3]. In analysis, the wind load on the container cannot be neglected in case large error will be produced. Therefore, wind load is applied on the entire

vehicle-bridge system and influences the coupled vibration. Meanwhile, the coupled vibration varies with mean wind velocity and the vehicle speed. Displacement and acceleration of the vehicle and bridge increase with the mean wind velocity, especially in the lateral direction.

(2) Vehicle-bridge coupled vibration response under seismic and operational wind load

One typical seismic code, such as EI Centro wave was applied to the vehicle-bridge system and neglected multi-point excitation and traveling-wave effect. In simulation, mean wind velocity and lateral seismic acceleration were taken 20m/s and 0.34g respectively, because that Typhoon (or storms, hurricanes) and earthquake this two kinds of extreme external environment excitation occur at the same time is very unlikely. The starting point is properly selected to assure the occurrence of maximum acceleration. On full rigid supports, when the vehicle is running at 4m/s in two line way, the vertical and lateral displacement and acceleration in the middle of the bridge with and without seismic load are compared in Figure 11 a), b), c).

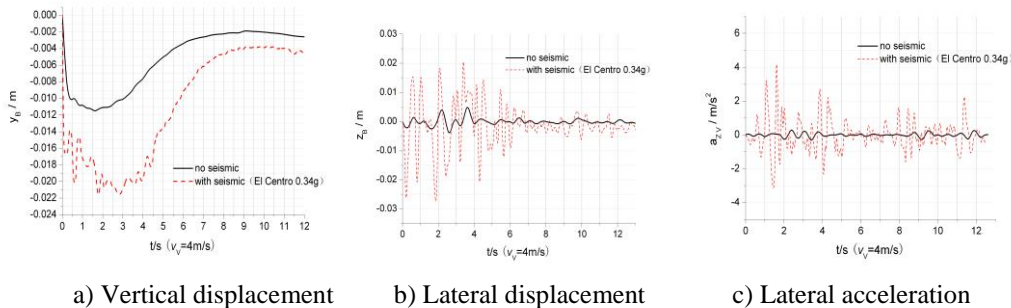


Figure 11. The Dynamic Response Comparison of the Vehicle-bridge Vibration under either Seismic Load or Not

Figures 11 presents that when seismic load applied, the maximum response and frequency value become larger than that without earthquake load. For example, the displacement and acceleration in middle span under seismic load is 1.9, 4.6 and 12.4 times than that without. Furthermore, vertical displacement time-history in middle span presents moving vehicle load is significant for the coupled vibration and that seismic load mainly affects the amplitude. However, in lateral vibration analysis, all time-history curve is similar to EI Centro wave, which state that seismic load is main cause, compared to operational wind load and self-excitation. Therefore, if the construction site probably suffers from rarely occurred earthquake, seismic load must be considered in the design.

4. Structural and Running Safety Assessment of the Vehicle-bridge System

4.1. Structural and Running Safety Assessment under Wind Load

When vehicles double-running, both vertical static deflection y_s and lateral static deflection z_s vary with the mean velocity \bar{U} illustrated in Table 3. From Table 3, static vertical and lateral deflections and dynamic deflections comply with TB10002.1-99.

Table 3. Maximum Vertical and Lateral Static Deflection, Wheel-Rail Relative Displacement vs. Mean Velocity of the Fluctuating Wind (the truss bridge rigid supported)

\bar{U} / m/s	20	25	30	35	40	45	50	55	60
y_s / mm	10.1	10.2	10.3	10.5	10.6	10.8	10.9	11.0	11.1
z_s / mm	4.14	4.53	5.02	5.59	6.25	7.00	7.84	8.77	9.78
$ \mu_s $ / mm	10.3	10.8	11.6	12.1	12.7	13.2	13.9	15.0	15.5
$ \Delta $ / mm	5.94	6.90	8.15	9.55	11.0	12.4	14.1	16.6	19.2

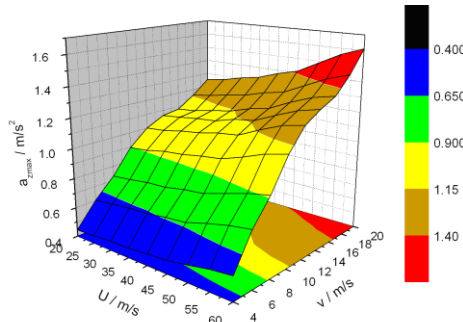


Figure 12. Maximum Lateral Acceleration Response of the Truss Bridge vs. v_v and \bar{U}

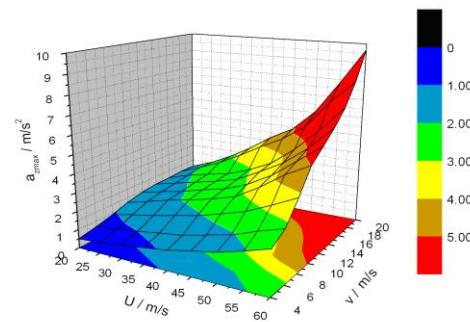


Figure 13. Maximum Lateral Acceleration Response of the Vehicle vs. v_v and \bar{U}

Figure 12 presents that lateral acceleration of the bridge increases with the vehicle speed and wind velocity. So does the vertical acceleration. When the vehicle speed and mean wind velocity are 20m/s and 60m/s respectively, vertical acceleration reaches 2.43m/s².

According to acceleration standard, vertical acceleration value is below 0.5g. However, when wind velocity is larger than 45m/s and the vehicle speed larger than 20m/s, or when wind velocity is larger than 55m/s and the vehicle speed larger than 18m/s, the lateral acceleration is beyond the limit, 0.14g by TB10002.1-99 standard.

Vertical and lateral relative displacement maximum can be referred in Table 3. According to derailment geometric condition, $|\mu_s| \geq 25\text{mm}, |\Delta| \geq 37.5\text{mm}$, when wind velocity is below 60m/s and vehicle speed below 20m/s, the vehicle is safe. It is noted that wheel-rail relative displacement errors do exist and thus stationarity indicator must be examined further.

From Figure 13, lateral acceleration rises with the two velocities. When the vehicle speed and mean wind velocity are 20m/s and 60m/s respectively, vertical acceleration reaches 9.68m/s². Vertical acceleration satisfies the similar trend and its maximum is 2.31m/s², far below the lateral value.

According to the vehicle running stationarity assessment standard, vertical acceleration maximum is out of reach of the threshold 0.7g by GB5599-85 standard. However, when wind velocity is larger than 50m/s and the vehicle speed larger than 18m/s, or when wind velocity is larger than 55m/s and the vehicle speed larger than 14m/s, the lateral acceleration is beyond the limit, 0.5g by TB10002.1-99 standard.

In summary: (1) Deflection-span ratio and acceleration indices are suggested to assess the bridge safety. That is, deflection-span is examined first, acceleration indices next. (2) Lateral acceleration of the vehicle and bridge probably go beyond the threshold, especially for the vehicle. (3) When the vehicle runs at the designed speed of 4m/s and mean wind velocity less than 60m/s, indicators are far less than the standard limit, which indicates the structural safety

and running stationarity are good. And when on full rigid supports, the vehicle velocity can be raised to 8m/s.

4.2. Structural and Running Safety Assessment under Seismic and Operational Wind Load

By the El Centro wave excitation, lateral acceleration maximum trend of the vehicle and the middle span of the truss bridge on two kinds of supports vs. seismic intensity and the vehicle speed are shown in Figure 14 and Figure 15.

Comparing Figure 14 and Figure 15 to Figure 12 and Figure 13, the sensitivity of the response to the seismic load is greater than the wind load. Illustrated in Figure 13 and Figure 14, safety zone of taking lateral acceleration of bridge as assessment indicator is smaller than that of the vehicle, which indicates that the bridge suffers more serious from seismic load. In contrast, Figure 12 and Figure 13 reflect the opposite regulation, which means the vehicle suffers more serious from wind load. That's because ground motion is from the ground upwards while containers on the vehicle have a large frontal area. Meantime, LRB can obviously enlarge the safety zone.

By the El Centro wave excitation, when the vehicle speed is 4m/s, seismic intensity threshold of the bridge on full rigid or flexible supports are 0.16g and 0.33g; when the vehicle speed reaches 6m/s, seismic intensity thresholds of the bridge change to 0.10g, 0.20g; when the vehicle speed ranges from 8 to 10 m/s, the thresholds reduce to 0.05g and 0.10g; at last, when the vehicle speed ranges from 10 to 20 m/s, the thresholds reduce to 0.05g and 0.05g again.

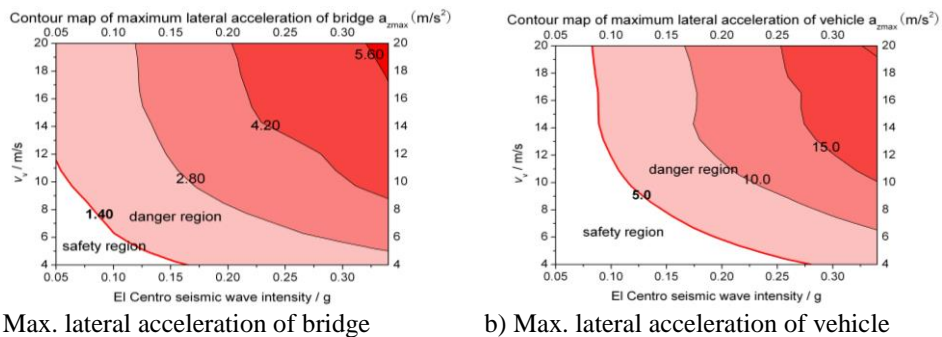


Figure 14. Ground Motion Intensity and Vehicle speed Limits when Rigid Supported by El Centro Seismic Wave

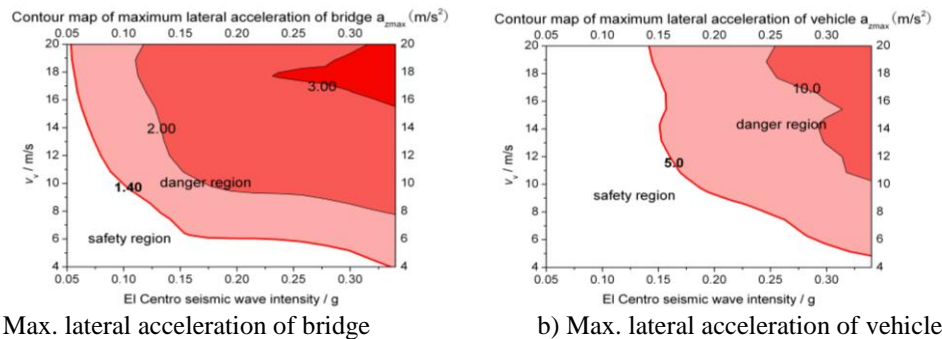


Figure 15. Ground Motion Intensity and Vehicle speed Limits when LRB supported by El Centro Seismic Wave

By the San Fernando wave excitation, full rigid or flexible supporting formulation, Figure 16 and Figure 17 show safety values for the ground motion intensity of the vehicle-bridge system and speed limitation of the vehicle.

By the San Fernando wave excitation, the results of the vehicle-bridge coupled vibration vary with the ground motion intensity, the speed of vehicle and supports in the form of change regulation and trends, which also applies to the case inspired by the EI Centro waves, but the values of the two waves are in distinction. By the EI Centro wave excitation, when the vehicle speed is 4m/s, seismic intensity threshold of the bridge on full rigid or flexible supports are 0.4g and 0.5g; When the vehicle runs at the speed of 6m/s, the values are 0.2g and 0.35g; When running at 8~10m/s, resulting in 0.1g, 0.2g respectively; When it is 10~20m/s, the outcome is 0.1g; In general, the threshold values calculated by the EI Centro waves are bigger than San Fernando.

Because the predominant period of the two waves is 0.5s for EI Centro wave and 0.2s for San Fernando wave, and the inherent frequency of truss bridge lays between 1~2Hz, besides EI Centro wave lasts longer, although the ground motion intensity of San Fernando wave is larger, instead the vibration response is slower than EI Centro. This illustrates that structure (vehicle) safety limitation value is related to the seismic characteristics.

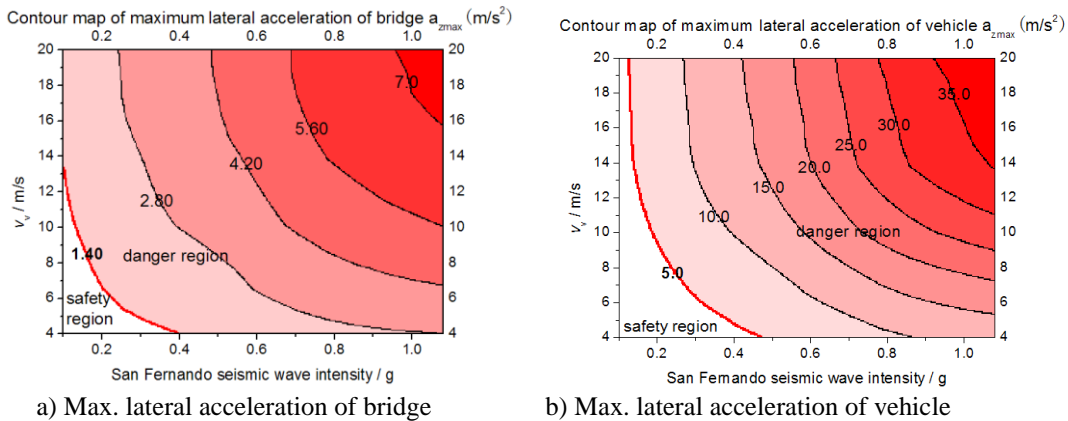


Figure 16. Ground Motion Intensity and Vehicle Speed Limits when Rigid supported by San Fernando Seismic Wave

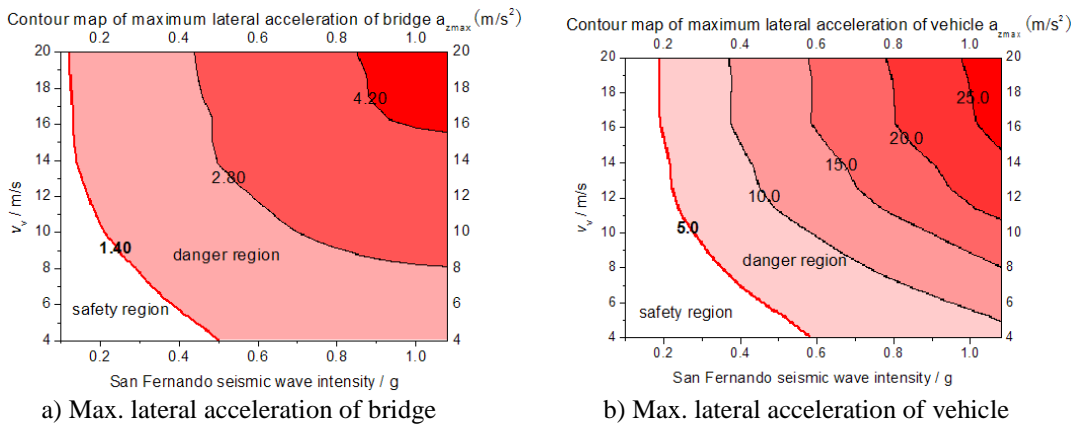


Figure 17. Ground Motion Intensity and Vehicle Speed Limits when LRB supported by San Fernando Seismic Wave

Due to the fact that the predominant period of El Centro wave is near to the first order natural frequency of the truss bridge, the seismic intensity and the vehicle speed limit under the El Centro excitation can be considered as the designed safety threshold. Furthermore, full LRB flexible support is suggested as the truss bridge support type. In conclusion, a safety factor is taken into account, when the seismic intensity is below 0.3g, 0.2g, and 0.1g, 0.05g, the vehicle speed limit is suggested to be 4m/s, 6m/s, 8m/s, 20m/s respectively.

The above analyses were based on the conditions that the vehicles were running on the bridge during earthquake. Assume the vehicle stops in the position of middle span, still input El Centro wave and operational wind load, when LRB supported, the vertical and lateral deflection meets TB10002.2-2005 provisions. Therefore, ground vibration acceleration monitoring sensor can be set in the automated terminal, when the intensity limit reaches, the container vehicle decelerate to stop immediately to ensure the safety of the structure.

5. Conclusion

(1) In the proposed ACT scheme, the safety and running stationarity of container vehicle-truss bridge structure directly affects the efficiency and life span of the three dimensional container handling and distributing system. When assessing the structural safety, it is suggested that first evaluate by deflection-span ratio, then, then acceleration indices can be used to assess further. As for running safety and stationarity, lateral acceleration indices is recommended.

(2) The dynamic response results of scale model test and prototype simulation of self-excitation container vehicle-truss bridge coupled vibration prove with each other, which confirms the method of applying free-interface CMS to solve vehicle-bridge coupled vibration problem and the method of introducing model test to validate large scale structure dynamic response, also validates LRB's effects on vibration isolation.

(3) In this case, vertical coupled vibration of the container vehicle-truss bridge system is caused mainly by the vehicle moving load, and self-excitation is a major factor. This differs from that the lateral response is mainly controlled by wind power in the case of long-span bridge on high speed railway. Wind, seismic load will greatly enhance the lateral vibration. As vehicle speed, fluctuating wind average velocity or ground motion intensity increases, the response increases. And the sensitivity of the response to the seismic load is greater than the wind load.

(4) The truss bridge is suggested to use LRB supported. Thus, under wind load (wind velocity<60m/s) without earthquake, the vehicle can reach 20m/s. Moreover, under operational wind (wind velocity=60m/s) and ground motion (EI Centro wave) excitation simultaneously, when the seismic intensity is below 0.3g, 0.2g, 0.1g, 0.05g, the vehicle speed can reach up to 4m/s, 6m/s, 8m/s and 20m/s respectively. However, when the intensity is up to 0.3g, the vehicle must be stopped at once.

Acknowledgements

This work is sponsored by Shanghai Top Academic Discipline Project- Management Science & Engineering, this paper is supported by Doctoral Fund of the Ministry of Education Jointly Funded Project (20123121120002), Quality Standards and Metrology Research Project of the Ministry of Transport (2013-419-899-040) and Shanghai Education Committee Project "Shanghai Young College Teacher Training Subsidy Scheme", also supported in part by Ministry of Transport Research Projects (2012-329-810-180), Shanghai Municipal Education Commission Project (12ZZ148, 12ZZ149, 13YZ080).

References

- [1] X. He, X. Youlin and Y. Quansheng, "Dynamic response of longspan suspension bridge to high wind and running train", Journal of the China Railway Society, vol. 24, no. 4, (2002), pp. 83-91 (In Chinese).
- [2] X. Y. L., Z. Nan and X. He, "Vibration of coupled train and cable-stayed bridge system in cross wind", Bridge Engineering, the American Society of Civil Engineers (ASCE), vol. 26, no. 1, (2004), pp. 1389-1306.
- [3] G. Weiwei, X. He and X. Youlin, "Dynamic response of long span suspension bridge and running safety of train under wind action", Engineering Mechanics, vol. 23, no. 2, (2006), pp. 103-110 (In Chinese).
- [4] G. Xiangrong and Z. Qingyuan, "Analysis of critical wind speed for running trains on a schemed Yangtze River bridge at Nanjing on Jing-Hu high speed railway line", Journal of the China Railway Society, vol. 23, no. 5, (2001), pp. 75-80, (In Chinese).
- [5] L. Yongle, Q. Shizhong and L. Haili, "Study on wind velocity field for the coupling vibration of wind-vehicle-bridge system", Acta Aerodynamica Sinca, vol. 24, no. 1, (2006), pp. 131-136, (In Chinese).
- [6] H. Yan, X. He and Z. Nan, "Dynamic response analysis of Train-Bridge system under non-uniform seismic excitations", China Railway Science, vol. 27, no. 5, (2006), pp. 46-53, (In Chinese).
- [7] Y. B. Yang, "Vehicle-bridge interaction analysis by dynamic condensation method", Structural Engineering, the American Society of Civil Engineers (ASCE), vol. 121, no. 11, (1995), pp. 1636-1643.
- [8] L. Kailiang, Q. Huiqing and M. Fei. "Free-interface component mode synthesis technique with link substructure as super-element", Journal of Tongji University (Natural Science), vol. 38, no. 8, (2010), pp. 1215-1220, 1233, (In Chinese).
- [9] X. He and Z. Nan, "Vehicle and structure dynamic interaction(2nd edition)", Science Press, Beijing, (2005).
- [10] M. Shinozuka and C. M. Jan, "Digital simulation of random process and its application", Journal of Sound and Vibration, vol. 25, no. 1, (1972), pp. 111-128.
- [11] H. A. Capers and M. M. Valeo, "FHWA's International Scan on Ensuring Bridge Safety and Serviceability", Transportation Research Record: Journal of the Transportation Research Board, vol. 2202, no. 4, (2010), pp. 117-123.
- [12] S. S. Law and J. Li, "Updating the reliability of a concrete bridge structure based on condition assessment with uncertainties", Engineering Structures, vol. 32, no. 1, (2010), pp. 286-296.

Authors



LU Kai-liang, received his PhD from Tongji University, Shanghai, China. Currently, he is working in Logistics Engineering College, Shanghai Maritime University (SMU) as a lecturer. His research interests include port machine structure and system dynamics, theory and method of dynamic design and optimization of structure, *etc.* He has 16 publications to his credit both in international and national Journals. He is a committee member of Shanghai Society of Theoretical & Applied Mechanics, member of China Construction Machinery Society (CCMS), and Logistics Engineering Institution, CMES.

